METAL BELLOWS MECHANICAL FACE SEALS FOR HIGH PERFORMANCE PUMP APPLICATIONS

by

Amit Datta

Director, Group Research and Development

James F. Gardner

Manager, Product Technology, Group Research and Development

James U. Derby

Manager, Materials Characterization, Group Research and Development

and

David P. Casucci

Enginering Services Manager, Process Sealing Division

EG&G Sealol, Fluid Components Technology Group

Cranston, Rhode Island

Amit Datta is Director of Group Research and Development in the EG&G Sealol Fluid Components Technology Group. At EG&G, he is responsible for Fluid Components Technology, group-wide Research and Development, and new product development.

Prior to joining EG&G, Dr. Datta was Manager of Product Development at Metglas Products, a division of Engineered Products, Allied Signal. His research background is primarily on advanced materials and processing. He has published over thirty papers in conference proceedings and technical journals, in the area of materials technology. He is a member of ASM, STLE, ACS, and AWS.

James F. Gardner is Manager of Product Technology in Group Research and Development for the EG&G Sealol Fluid Components Technology Group. He has a BSMAE degree from Illinois Institute of Technology.

As the Manager of Product Technology, his responsibilities include design, analysis, and performance testing of new products.

Mr. Gardner has 27 years experience in seal research, fluid mechanics, analysis, fluid film bearings, and heavy machinery such as pumps and centrifugal gas compressors. In the area of seals, he developed dry running spiral groove gas face seals for high pressure compressor applications and performed research on contract for the A.E.C., on cover gas seals for liquid sodium pumps for breeder reactor applications. Mr. Gardner was affiliated with Crane Packing Company (Project Engineer, Research) and Ingersoll-Rand Research (Member of Technical Staff), prior to joining Group Research at EG&G Sealol.

Mr. Gardner has four technical publications to his credit. He is a member of STLE, and ASME.
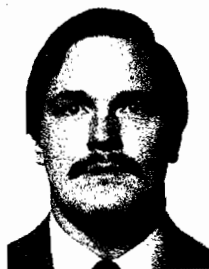
James U. Derby is Manager of Materials Characterization for Group Research and Development at EG&G Sealol Fluid Components Technology Group. He has a M.S. degree in Ceramic Science from Alfred University and a B.A. degree in Physics from Thiel College.

Mr. Derby's research interests lie in the microstructural/tribological property relationships for materials including ceramics, carbon graphites, and coatings. His responsibilities include optimization of processing conditions and development of specifications for new materials.

Mr. Derby was a Senior Research Engineer with the Research and Development Center of Standard Oil (Carborundum). He was responsible for tribology and corrosion research on advanced ceramic materials used for high temperature and wear applications.

Mr. Derby has eight technical publications and presentations to his credit. Mr. Derby holds membership in the STLE, ACE, and ASM.

David P. Casucci is Engineering Services Manager in the Process Sealing Division of EG&G Sealol in Cranston, Rhode Island. Mr. Casucci has a B.S. degree in Mechanical Engineering and Applied Mechanics from the University of Rhode Island.

His responsibilities include the application, design and development of metal bellows seals for pumps and rotating equipment.

Since joining EG&G Sealol in 1978 as Product Engineer, he has held positions in Engineering and Customer Service at different EG&G Sealol divisions.

Mr. Casucci is a member of the STLE.

ABSTRACT

Metal bellows seals have been steadily gaining wider acceptance in process and general industrial pump applications. This paper discusses design criteria and advantages of metal bellows seals, and attempts to define applications where the metal bellows seals offer operating advantages.

The design principles of metal bellows seals to adjust hydraulic balance, or mechanical face contact force are explained. The mechanical face contact force, and not balance, is considered to be the important design criterion.

The significance of welded metal bellows plate (diaphragm) shape is highlighted, and the optimum plate configuration for fatigue strength, manufacturability, and pressure capability is discussed.

To further enhance the reliability of metal bellows seals, it is critical to control the seal face distortion and tribological behavior of the wear pair. The role of finite element analysis as a design tool to minimize face distortion and the microstructural control of the seal face materials to minimize face friction and wear are discussed.

INTRODUCTION

Balanced seals using metal bellows as secondary seals were first introduced in the 1950's for high temperature industrial pump applications [1]. Since then, metal bellows seals have been steadily gaining a wider acceptance in process and general industrial pump applications. Although pusher-type seals, using o-ring or other secondary seals, can operate at higher pressures, welded metal bellows seals are better for high temperature, abrasive applications, and prevent hangup of the secondary seal caused by fretting and by particulate matter. Welded metal bellows seals typically handle a wide range of temperatures ($-180°$ to $+800°F$) and pressures up to 1000 psig or higher in typical industrial pump sizes [2].

There are both similarities and differences between pusher-type and metal bellows seals. Both seals can be hydraulically pressure balanced to minimize the mechanical contact force. Both seals may be designed with either a rotating or stationary head. With typical pump applications (1750 to 3600 rpm), a rotating seal head arrangement is often used to simplify installation. A stationary seat is mounted in the casing, and a rotating head is installed over the shaft, and locked to the proper working length. For high speed applications, stationary heads are typically used for both types of seals. To minimize dynamic tracking problems, the rotating components are made as simple as possible. This, however requires a more elaborate attachment to the rotating shaft.

The major difference between metal bellows seals and pusher-type seals is in the secondary seal. A typical balanced pusher-type seal is shown in Figure 1. The dynamic secondary seal is usually an O-ring, or Teflon™ wedge assembly, that moves axially to compensate for face wear, shaft thermal growth, or shaft runout. Springs are used to ensure face contact at zero pressure. Typically, a single large diameter coil spring, a plurality of small coil springs, or a wave spring is used to ensure face contact at low pressures or startup. At high pressures, hydraulic forces dominate. A stepped face and a stepped shaft or sleeve are necessary to hydraulically balance the pusher seal to minimize face loading.

A typical metal bellows seal configuration is shown in Figure 2. The bellows core acts as both the spring, and the dynamic secondary seal. The bellows core flexes to accommodate axial motion and runout. The seal is mounted to the shaft with the use of other static secondary seals. These are usually o-rings, or graphitic packings, selected commensurate with the tempera-

①–DYNAMIC SECONDARY SEAL
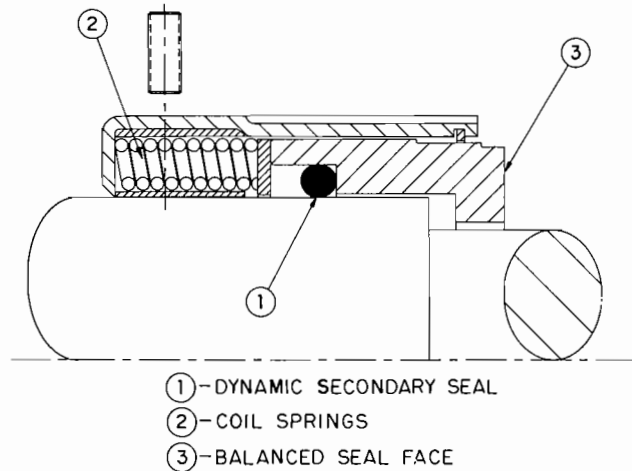②–COIL SPRINGS
③–BALANCED SEAL FACE

Figure 1. Typical Balanced Pusher Seal.

ture and corrosive environment requirements. These static seals do not have to flex. All flexing action takes place within the metal bellows, which is hermetically welded at the ID and OD of each bellows plate.
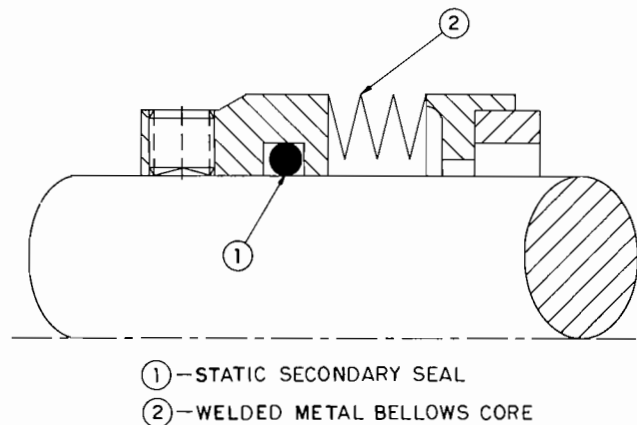

①–STATIC SECONDARY SEAL
②–WELDED METAL BELLOWS CORE

Figure 2. Typical Welded Metal Bellows Seal.

There is no visible step in a metal bellows seal. Metal bellows seals are hydraulically balanced by locating the effective diameter of the bellows with respect to the face. This will be discussed in a later section.

There are a number of advantages of metal bellows seals. Because of the dynamic elastomeric secondary seals, pusher-type seals have a restricted service temperature range determined by the available o-ring seal materials. Attempts have been made to use a filament graphite wedge arrangement as a sliding secondary packing to extend the temperature limit of pusher seals to 750°F with limited success [3].

In addition to limiting the temperature range, dynamic secondary seals can also cause shaft fretting due to reciprocating axial motions. Fretting is further exacerbated in a corrosive environment due to fretting corrosion. The hangup problem is also encountered in concentrated slurry applications caused by clogging at secondary seals or springs. Metal bellows seals eliminate the need for dynamic secondary packings and their associated problems. There is no fretting or hangup problem with welded metal bellows seals. The temperature limitations are as high as the rated temperature of static filament graphite packing

(800°F). In some cases, metal-to-metal secondary seals have proved to be successful above 850°F.

The advantages of metal bellows over pusher type seals in typical refinery applications are well documented in the literature. In high temperature applications (500°F to 700°F), metal bellows seals without cooling systems offer an appreciably longer life than that of pusher type seals [4, 5]. Similarly, in abrasive applications, the performance of metal bellows seals is far superior to that of pusher seals which suffer from hangup problems associated with secondary elastomeric seals [6, 7, 8].

In refineries, seal failures constitute the major cause of breakdown of rotating equipment. By replacing pusher type seals with metal bellows seals in a refinery in France, the maintenance cost was reduced by about 50 percent. The average seal life span was almost doubled [9].

More detail follows on bellows seal design based on mechanical contact force, as effected by hydraulic balance and face distortion. The application of finite element analysis (FEA) to minimize face distortion is discussed. The significance of bellows plate (diaphragm) configuration and microstructural control of seal face materials are also addressed.

EXPERIMENTAL DETAILS AND DISCUSSION OF RESULTS

Hydraulic Balance and Face Loading of Metal Bellows Seals

Pusher Type Seal

The design principle of a balanced pusher type seal is illustrated by a free body diagram in Figure 3. It should be that the fluid pressure acts on an area A on the back of the seal, thereby exerting a closing force; and on an area A on the face of the seal, tending to open the seal. The ratio A_c/A_o is commonly referred to as the hydraulic balance (B) of the seal. In addition to the two fluid pressure forces, there are two mechanical forces acting in opposite directions on the seal. These are the spring force, F_s, and the mechanical contact force, F_{mc}.

At equilibrium,

$$F_{mc} + KPA_o = PA_c + F_3 \qquad (1)$$

where,

P = fluid pressure (lbs/sq in)
K = pressure gradient factor (dimensionless)

Dividing (1) by the seal face area A_o, the seal face contact pressure (P_{mc}) is given by,

$$P_{mc} = P(B - K) + P, \qquad (2)$$

where,

$$P_3 = F_3/A_o \text{ (lbs/sq in)}$$

The value of K is between 0.0 and 1.0, where 0.0 would represent no fluid pressure across the face outer diameter/OD contact) and 1.0 would be fu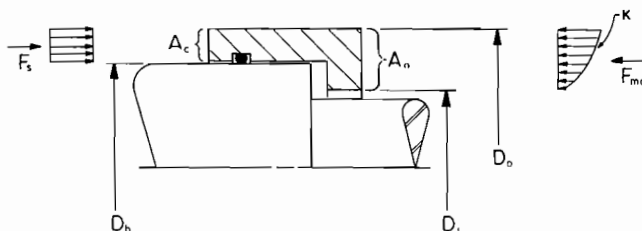ll system pressure across the face (inner diameter/ID contact). Parallel seal faces have a linear pressure distribution, for which K = 0.5. For this case, with B = 0.5, the face pressure (Pmc) equals the value of spring pressure (Ps), thereby, cancelling the effects of hydraulic loading. However, if the faces become convergent (ID contact), K will be >0.5, and the faces will separate. Hence, to ensure face closing, a minimum balance ratio of 0.6 is generally used. A common practice is to choose a balance ratio of 0.65 to 0.75 [10].

It is important to note that, through the choice of a proper balance ratio, face contact pressure P_{mc} can be optimized to reduce friction and wear at the seal face. However, an optimum value of P_{mc} is difficult to define as it depends on the seal system characteristics consisting of face materials, the fluid and operating conditions. For typical pump applications, a commonly used maximum value of P_{mc} is about 200 psi [10].

From Figure 3,

$$B = \frac{A_c}{A_o} = \frac{D_o^2 - D_b^2}{D_o^2 - D_i^2} \qquad (3)$$

Therefore, to adjust seal balance B, the balance diameter D_b (or the ID of the dynamic secondary seal) is designed to be greater than D_i. For any given face geometry B is constant with respect to pressure. By considering K constant, P_{mc} is a linear function of pressure.

Bellows Seal

A free body diagram of a bellows seal with the attendent fluid pressure and mechanical forces is shown in Figure 4. The balance diameter D_b, as defined for the pusher seal, does not physically exist. The hydraulic balance B is no longer constant and changes with pressure as the bellows convolutions tend to collapse, as schematically shown in Figure 5.

However, to comply with pusher seal design principles and select a desired value of B, an Effective Balance Diameter (EBD) can be derived from the bellows closing force (F_b), due to pressure only. Referring to Figure 4:
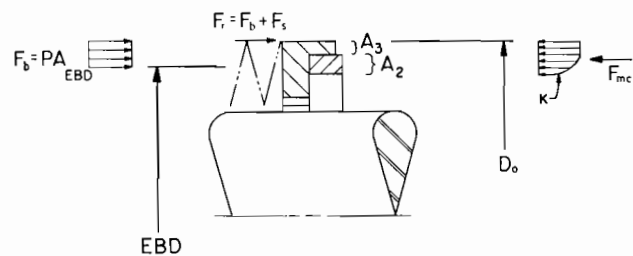
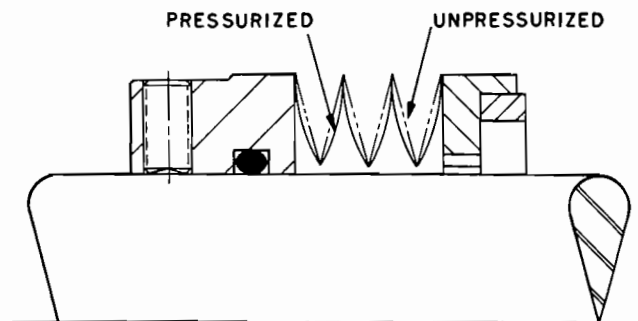

Figure 4. Free Body Diagram of Welded Metal Bellows Seal.

Figure 5. Schematic Representation of Bellows Convolution Collapse under Pressure.

Figure 3. Free Body Diagram of Pusher Seal.

$$F_b = F_r - F_s$$

where,

F_r = bellows total reaction force (lbs)
F_s = bellows spring force (lbs)

and

$$EBD = \sqrt{D_o^2 - \frac{4}{\pi P} F_b} \qquad (4)$$

where,

D_o = bellows O.D. (in)
P = fluid pressure (lbs/sq in)

At $P = 0$, Equation (4) is not valid and cannot be used to derive an EBD. The EBD at $P = 0$ is generally assumed to be the mean diameter of the bellows span [11].

Without invoking the concept of EBD, a more direct analysis of P_{mc} can be made from bellows total reaction force F_r. From Figure 4,

$$F_r = PA_3 + KPA_2 + F_{mc}$$

or,

$$P_{mc} = \frac{F_r}{A_2} - P\left(\frac{A_3}{A_2} + K\right) \qquad (5)$$

where,

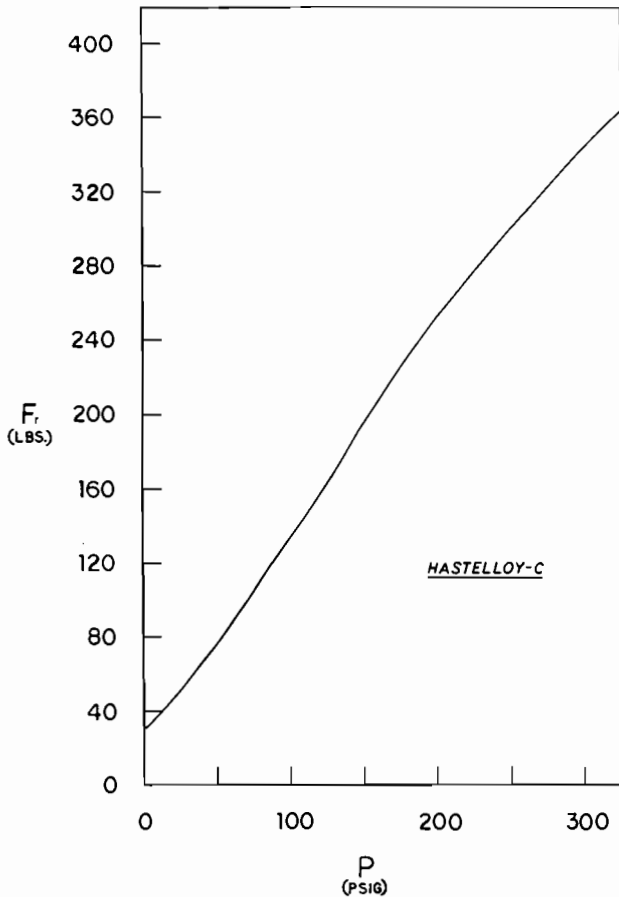$$P_{mc} = \frac{F_{mc}}{A_2} \quad \text{(lbs/sq in)}$$

The values of P_r are determined experimentally as a function of pressure. A typical curve is shown in Figure 6. Using experimentally determined values of F_r as a function of pressure and choosing appropriate dimensions of A_2 and A_3, the face contact pressure P_{mc} is adjusted to minimize wear.

The variation of P_{mc} with system pressure and K can be estimated for both pusher and bellows seals using Equations (2) and (5), respectively, as illustrated in Figure 7. For the pusher seal, using $B = 0.75$, $F_s = 25$ lb, face area = 0.83 square in, values of P_{mc} are estimated for three values of K, (0.5, 0.75, and 1.0). For comparison, similar design parameters are also used for the bellows seal (i.e., balance at 0 psig - 0.75, bellows spring force at operating length = 25 lb, and face area = 0.83 square in).

It is evident that, P_{mc} values vary with pressure for both pusher-type and bellows seals. However, for pusher seals, the variation is linear with a constant B and spring force. For a bellows seal, P_{mc} is nonlinear with respect to pressure, as determined by the bellows closing force *vs* pressure curves.

Bellows Plate Shape and Configuration

To optimize bellows plate shape for face seal applications, detailed theoretical and experimental studies were conducted by Hulbert, et al. [12, 13], and a program (NONLIN) was developed for estimating stresses and strains in bellows plates under both pressure and axial deflection loadings.

Two typical metal bellows plate shapes are illustrated in Figure 8. Individual plates are welded at both edges, ID and OD,

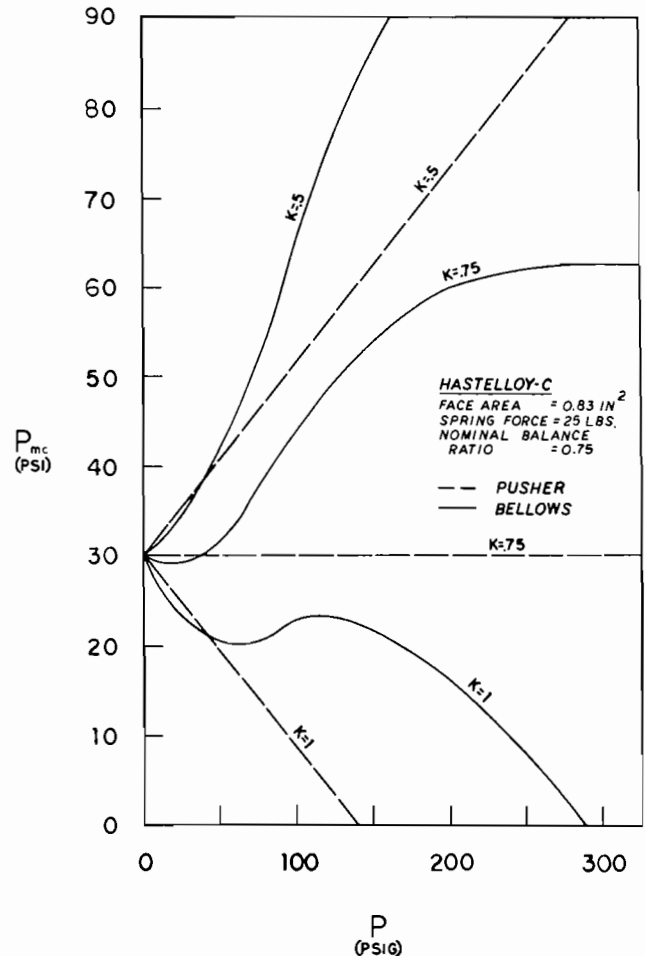Figure 6. Bellows Closing Force vs Pressure.

Figure 7. Face Mechanical Contact Force vs Pressure.

to form the bellows cores. One of the most common causes of seal failure stems from bellows fatigue in the vicinity of the weld. For externally pressurized bellows seals, the failure typically takes place at ID welds. If the flat portions of the bellows plates (Figure 8) are perpendicular to the bellows axis, the area in the vicinity of the weld is found to be the most highly stressed [12]. In addition, the areas in the vicinity of the welds also include heat-affected zones which have intrinsically weaker and variable microstructure than the original plate material. Therefore, for bellows with straight flat segments, the variability of the microstructure in the heat affected zones results in less reliable weld joints.
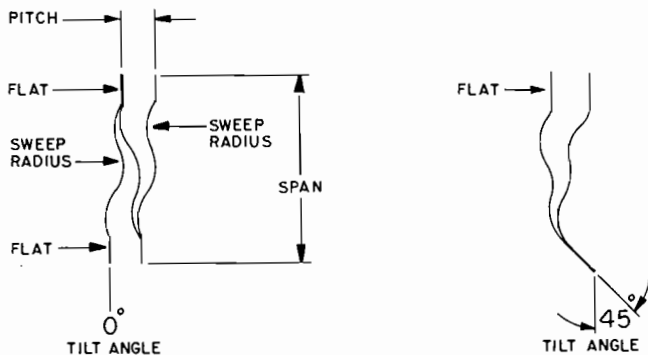

Figure 8. Flat Plate vs Curved ID plate.

By theoretical analysis [13] using linear, elastic, thin-shell theory, it was shown that tilting the bellows flats at an angle to the bellows axis could drastically reduce stresses at the welds and heat-affected zones. The analysis indicated that the stresses at the welds were predominantly bending stresses. With increasing tilt angles, the bending stresses are lowered. At the optimum tilt angle, close to 45 degrees, the bending stresses are minimized.

Following the analysis, Hulbert, et al. [13], experimentally verified that bellows cores with tilt angles close to 45 degrees had a superior fatigue resistance. Further, fatigue failures occurred at positions away from the welds. Elimination of fatigue failures at the welds, resulted in enhanced fatigue strength and reduced scatter in bellows fatigue life data.

The optimum 45 degree tilt-edge bellows plates, however, are more difficult to weld than the straight-edge or 0 degree tilt-edge bellows. Therefore, to improve manufacturability, the 45 degree tilt angle design is used only where it is necessary. For externally pressurized bellows seals with the bellows cores under compression, stresses at the OD tend to bend the plates towards each other; whereas; at the ID, the stresses tend to bend the plates away from each other. Because of these tensile bending stresses, the ID welds are generally subjected to fatigue failures. Hence, to improve the bellows fatigue life and manufacturability, a flat OD and a 45 degree tilt edge ID bellows plate shape, as shown in Figure 8, is preferred for OD pressurized bellows.

A number of seal manufacturers are now offering welded metal bellows with a wide variation of tilt angles at the ID. Typical tilt angles are 0 degree, 23 degrees, 30 degrees, and 45 degrees. Preliminary tests indicate that, at a moderately high pressure (500 psi) and under a cyclic loading (starts and stops at 150-300 psi), there is a lower propensity of fatigue failure as the tilt angle approaches 45 degrees.

Laminated or Multi-Ply Bellows Seals

With the optimum bellows plate shape, the pressure carrying capability of metal bellows is directly proportional to the plate thickness. However, as the plate thickness is increased, the spring rate also goes up as shown in Figure 9. These typical spring rate curves are determined by measuring axial deflections of bellows cores as a function of compressive loads on an Instron machine [11]. A high spring rate is undesirable as the bellows seals become less forgiving to installation errors. A slight change in operating length makes a drastic change in the face load. From Figure 9, it should be noted that, the spring rates of double-ply bellows are appreciably lower than those of single-ply bellows with twice the plate thickness. For example, the spring rate of a 0.003 inch, two-ply bellows is 358 lbs/in; whereas, that for a 0.006 inch single-ply bellows is 1453 lbs/inch.
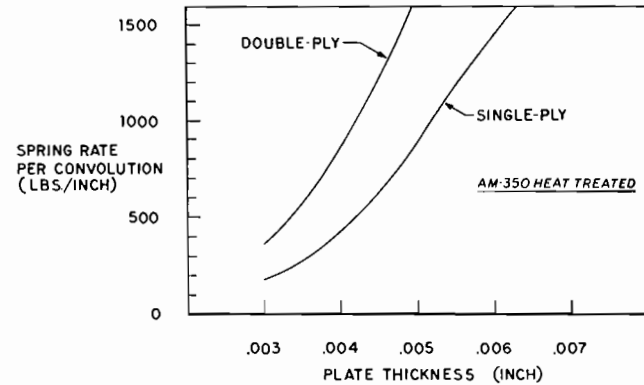

Figure 9. Spring Rates vs Plate Thickness, Single and Double-Ply Bellows.

One way to enhance the pressure carrying capability and simultaneously maintain relatively low spring rates is to fabricate metal bellows cores using a laminated (double-ply or multiply) construction [14]. A cross-section of a typical double-ply bellows core is illustrated in Figure 10. Enhanced pressure capabilities of double-ply bellows compared to single-ply bellows with twice the plate thickness can be illustrated by static rupture tests performed at the authors' laboratory. Static rupture tests were conducted using single-ply bellows cores with a plate-thickness of 0.008 in and double-ply bellows cores with a plate thickness of 0.004 in. The plate material was 410 stainless steel and bellows core geometry was kept constant. The results are shown in Table 1. The double-ply bellows seal with a 0 plate thickness 0.004 in exhibited an appreciable higher burst pressure than the single-ply bellows seal having a plate thickness 0.008 in. In addition to higher pressure capabilities, the double-ply bellows plates, as shown in Figure 10, are expected to make contacts during use and, therefore, are believed to be self-damping.

Table 1. Comparison of Static Burst Pressures of Single and Double-Ply Bellows Cores.

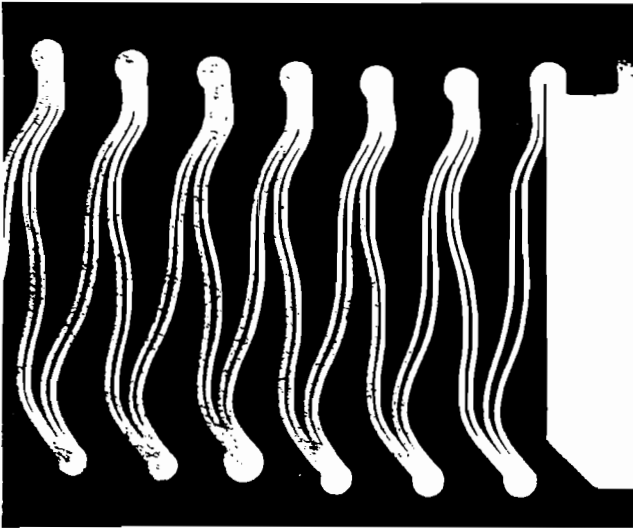| Size	Static Burst Pressure (psi)	
	Single-Ply, Plate Thickness 0.008 in	Double-Ply Plate Thickness 0.004 in
OD 1.0 in Span 0.25 in	8,800	14,000
OD 2.0 in Span 0.25 in	6,600	9,000

Plate Material — 410 Stainless Steel
Convolution — 10

Figure 10. Cross Section of Double-Ply Bellows Core.

Formed Bellows Seal

In addition to welded metal bellows, formed metal bellows seal plate shapes have also been optimized to withstand a greater pressure differential without increasing the plate thickness or spring rate and to minimize the variation of the hydraulic balance diameter [15]. The optimum bellows shape, as illustrated in Figure 11, consists of asymmetric crowns, the crowns of the convolutions directed towards the high pressure side of the seal being of greater radius of curvature than the crowns of the convolutions directed towards the low pressure side of the seal.
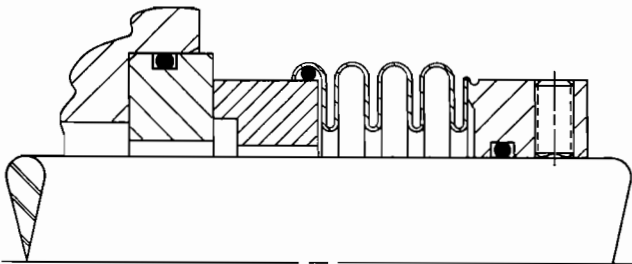

Figure 11. Typical Formed Metal Bellows Seal.

Commercially available formed bellows seals of the above configuration have been and are being evaluated at the authors' laboratory. They do exhibit higher spring rates than those of comparable welded metal bellows seals and are prone to variations in face loading due to normal installation errors. Presently, there are insufficient field data to evaluate the performance of the optimized formed bellows seals.

Welding Process Development

Fabrication steps of welded metal bellows is schematically shown in Figure 12. Stamped plates are first welded at the ID into single convolutions. Each convolution is then joined at the OD to form a core. For consistent bellows characteristics like spring rate, effective diameter and fatigue strength, it is necessary to follow a number of proprietary processes during stamping, welding and heat treatment. One of the important fabrication steps is welding, as special fixturing and critical welding

parameters need to be very accurately controlled to reproduce a consistently desirable weld bead geometry and microstructure. Usually, bellows plates are edge welded using Tungsten inert gas (TIG), microplasma, or laser welding processes [16]. To improve weld quality, minimize reject costs, and maximize welding rates, edge welding processes are usually automated, whereby welding parameters and bellows plate to arc geometries are maintained constant.
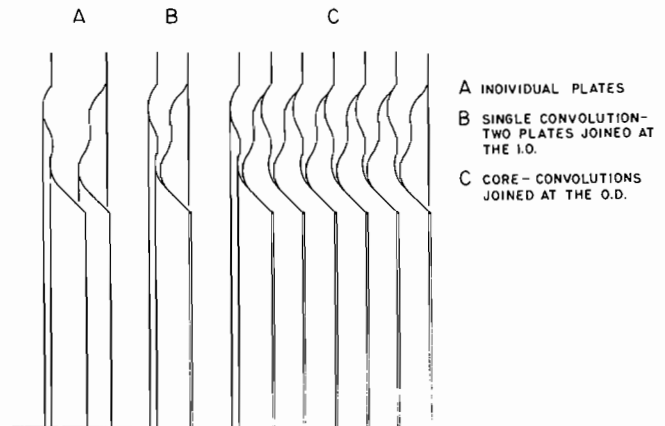

Figure 12. Schematic Representation of Bellows Core Welding Sequence.

High Volume/Lower Cost Bellows Seals

In addition to improving the quality of welded metal bellows, recent manufacturing developments have also focused on high volume/lower cost metal bellows seals for general sealing applications [17]. This high volume/lower cost product offers the advantage of metal bellows seals but with the equivalent price of conventional pusher-type seals. A high volume/lower cost metal bellows seal consisting of an alloy 20Cb3 bellows core and alloy 20Cb3 stamped end fittings is illustrated in Figure 13. Thus, expensive cast or machined parts are eliminated. Compared to the 300 series stainless steels, the alloy 20Cb3 provides improved resistance, weldability and mechanical stability. The drive through the rotor is by friction compression, which precludes the need to drill or predimple through the shaft or sleeve. Furthermore, the lower mass of the stamped end fittings, is expected to improve dynamic tracking of the seal ring because of its lower inertia.
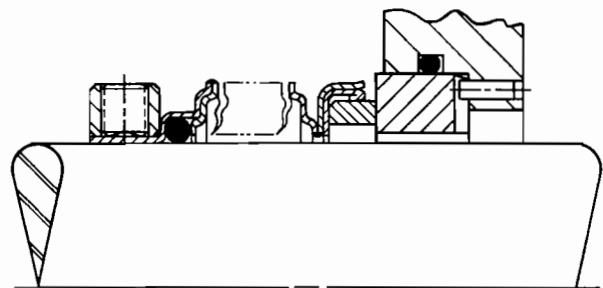

Figure 13. Typical Low Cost Welded Metal Bellows Seal.

Recently, these high volume/lower cost bellows seals have been cartridgized, as shown in Figure 14. This product is targeted for general industrial applications.
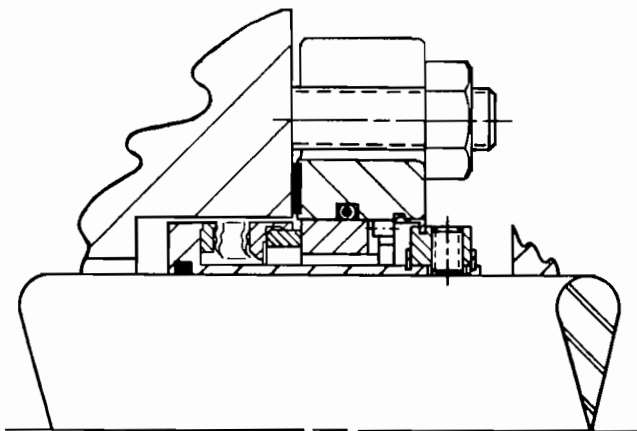
Figure 14. Typical Low Cost Cartridge Welded Metal Bellows Seal.

Bellows Fatigue

During use, the bellows core is subjected to continued axial flexing. Such flexing can occur from misalignment between rotating and stationary pieces and shaft vibration. In addition, the bellows core could also be excited to resonant vibration caused by pumping pressure pulsation, product flashing and dry running.

Although this resonant vibration can be damped by certain design features [18], the fatigue strength of the bellows material needs to be carefully evaluated. To prevent fatigue failures, accelerated tests are generally conducted under exaggerated conditions of pressure pulsation, axial stroking and shaft misalignment. Based on these data, fatigue life is extrapolated, assuming runout and pressure pulsation in normal pumping environments [11].

Seal Face Stability and Its Optimization

One of the uncertainties that affects the performace of mechanical seals is seal face contact pressure as defined by Equations (2) or (5). The desired seal face contact pressure, selected by controlling the hydraulic balance, will change as the pressure profile factor K is altered during operation resulting from seal and mating ring face distortions. Ideally, the faces are expected to remain flat or stable throughout the entire operating pressure and temperature ranges, thereby, maintaining designed contact pressure at the seal interface.

For the present state-of-the art metal bellows seals, the seal ring and mating ring inserts are generally shrink-fitted into metallic shells. This arrangement allows for several factors which tend to produce out-of-flat face conditions, as outlined below:

- shrink-fit induced distortion of the inserts
- pressure distortion of the entire shell, including the inserts
- thermal distortion due to heat generated at the face
- thermal distortion due to ambient temperature around the shell and insert combination

The first item, shrink-fit induced distortion of the insert, is a fairly dominant factor, as shrink-fit stresses are high as compared with stresses due to pressure loading. With standard designs, the insert distorts during the shrink fit operation; usually ID high. The face is than lapped flat. As the seal is heated for example, in a high temperature application, the shrink-fit stresses tend to decrease, and the insert distorts back. As the seal has been lapped, however, this now produces 0D high distortion, i.e., the formation of a diverging wedge between the seal faces.

This causes a low "K" value, and high mechanical contact stresses, as discussed under *Hydraulic Balance and Face Loading of Metal Bellows Seals.*

To minimize the above mentioned face distortion, it is necessary to optimize the shell-insert configuration using finite element analysis (FEA). The FEA allows us to estimate face distortions of various insert-shell assemblies and offers a design tool. A typical example is discussed below.

Finite Element Analysis

A nonlinear FEA code is being used to optimize shell insert configuration. The modelling of a typical nonoptimum retainer containing a carbon graphite insert is illustrated in Figure 15. The centerline of the assembly is to the left of the figure. In practice, the carbon graphite insert is shrink fitted into the metallic shell, which in turn, is welded to a metal bellows secondary seal. The point of attachment to the bellows is the weld preparation shown at the right center position of the figure.
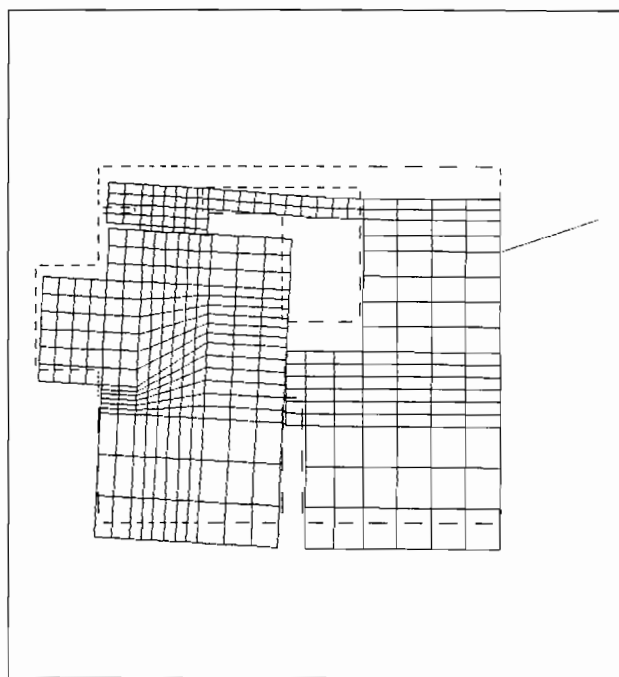

Figure 15. FEA Deflection Map as Shrink-Fitted.

The contact regions between the shell and the insert are modelled with gap friction interface elements. These elements represent two surfaces which may maintain or break physical contact and may slide relative to each other. These elements are capable of supporting only compression in the direction normal to the surfaces and model shear forces (Coulomb friction) in the tangential directions. Each of these elements has two different status conditions in each direction e.g., open/closed gap in the normal direction and sliding/not sliding interfaces in the tangential direction.

Hence, an iterative procedure is adopted to find the solution. Convergence occurs whenever the status of all the elements remains unchanged from the previous status.

Only the radial and axial distortion caused by the shrink are shown in Figure 15. The dotted lines show the original position; the solid lines show the position after the shrinkfit. The maximum radial deflection is 0.00923 in, as shown by the figure. Although, not shown in this paper, colored graphic maps of the stresses in both the insert and shell are also studied, as well as

deflection. Maps of radial stress, axial stress, hoop stress, or combined stress are analyzed, to optimize shell-insert designs.

The results of reheating the entire assembly to 320°F, are shown in Figure 16, to simulate a typical application. The contact stresses due to shrinkfit are now reduced, with a resulting effect on face deformation. Relative to the radial deformation, the face appears to be flat on this scale as shown in Figure 16. The actual face flatness, however, is shown by an enlarged plot of deflection across the seal dam nodes only, illustrated in Figure 17.
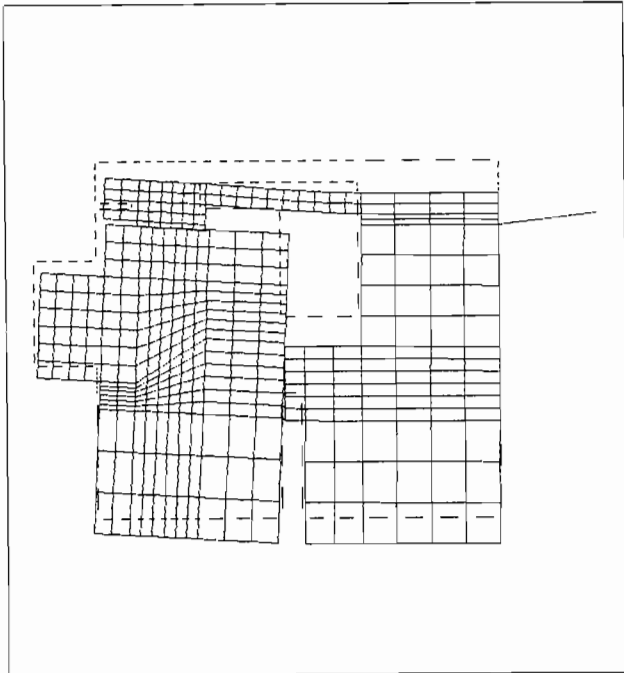

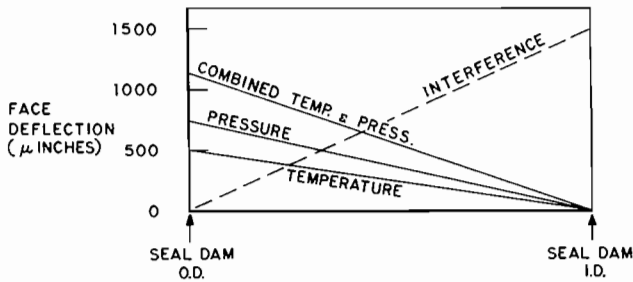Figure 16. FEA Deflection Map at 320°F.

Figure 17. Graphical Face Deflection Map.

The result of applying OD pressure to the assembly is shown in Figure 18. The pressure is assumed to exist about the entire body, with a linear (or other) pressure distribution across the seal dam. In addition, radial and axial reaction forces are applied at the point where the metal bellows core is attached. The amount of this force is a statically indeterminate quantity, as it depends on both metal bellows and shell relative distortions under pressure. Currently, high and low values are estimated for a sensitivity analysis to determine the effect of shell insert pressure deformation. Once again, we are most interested in face flatness, and stress distributions throughout the assembly. The corresponding face distortion due to OD pressure is also shown in Figure 17.
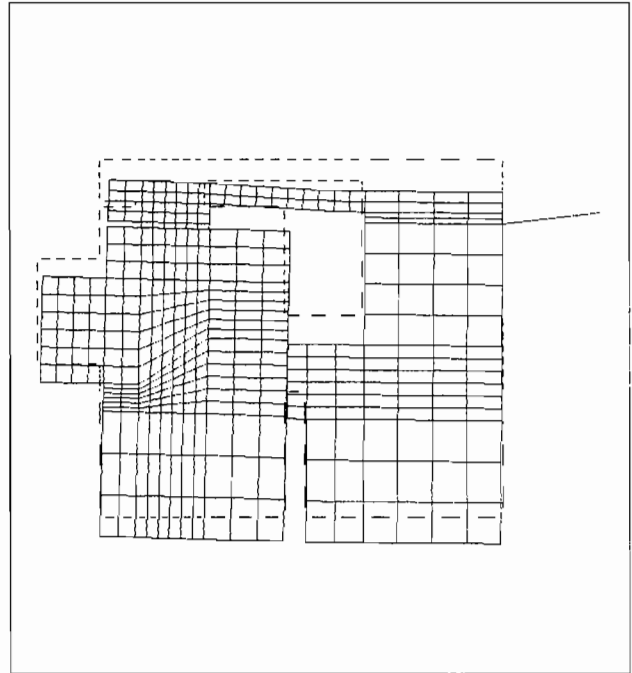

Figure 18. FEA Deflection Map at 700 PSI.

The assembly under the combined loading of pressure and temperature is shown in Figure 19. The temperature is assumed to be uniform throughout the assembly. The resulting face distortion across the seal dam is summarized again in Figure 17. In addition, although not shown herein, nonuniform thermal analysis is performed, showing for example, the effect of sliding frictional heat at the seal dam.
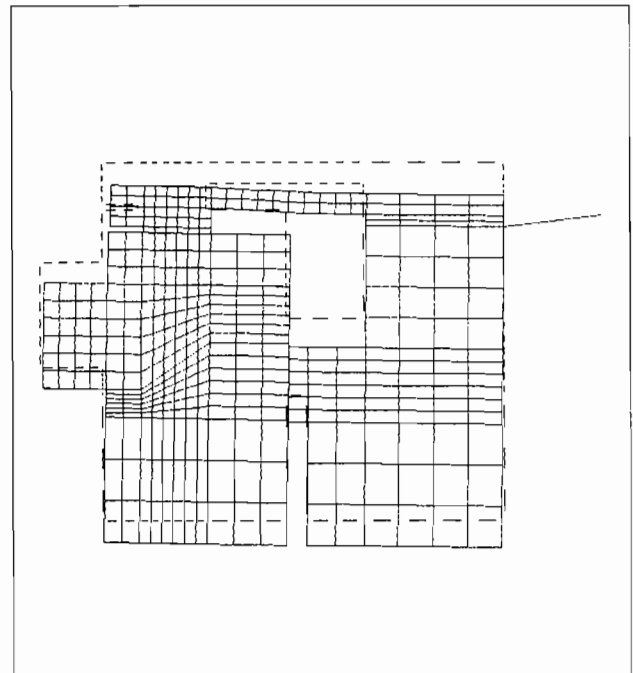

Figure 19. FEA Deflection Map at 320°F, 700 PSI.

One point of clarification as to Figure 17 would be useful. This figure is derived from the computer plots of deflection across the seal dam. The original shrink fit (shown by the dotted line) causes the seal face to distort 1500 microinches ID high, i.e., the ID of the seal would contact, if set on an optical flat. The seal, however, is then lapped flat. Thus, for the other plots (temperature only, pressure only, and combined loading), the 1500 microinch value is subtracted from the computer plots, to develop the actual seal face flatness.

Face distortion, shown in Figure 17, is very high, and is also in the wrong direction, i.e., OD high. This is typical of some of the problems encountered with non-optimum shell insert designs. FEA can be used as a design tool to minimize face distortion.

Experimental Determination of Face Distortion

To measure static seal face distortions as a function of seal OD pressure and ambient temperature, an optical flat test rig was designed and built. The test rig, shown schematically in Figure 20, consists of a very low expansion material optical flat, positioned over a test chamber. The test chamber can be pressurized up to 1000 psi, and also heated up to 750°F. By positioning a seal face against the optical flat, it is possible to accurately measure seal face distortions, caused by pressure and temperature. This allows for correlation of results as predicted by finite element analysis.
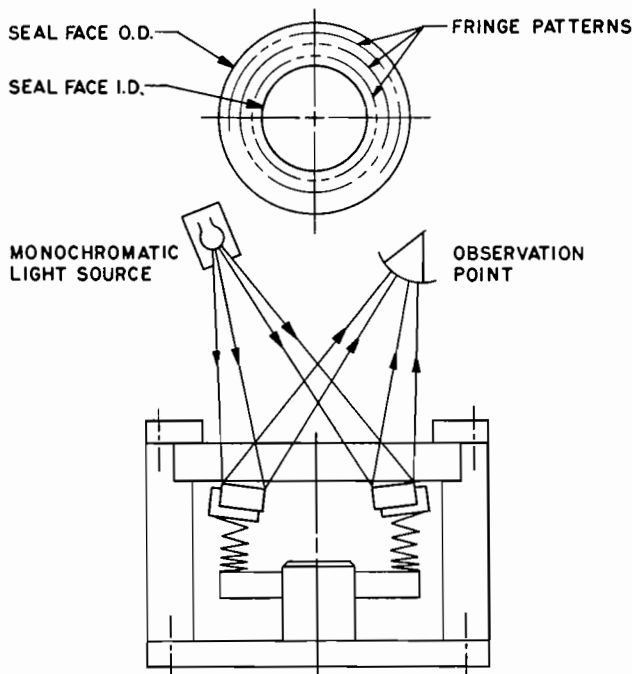

Figure 20. Face Distortion Test Rig.

Face distortion characteristics of typical commercially available metal bellows seals are summarized in Figure 21. It should be noted that the face distortions in Figure 21 reflect the effects of temperature only. The distortion at 400° is of the order of 90 μin or eight helium light bands.

Although actual face distortions under dynamic conditions, are somewhat different from the static distortions, the measurements provide important data to optimize the shell insert design for face stability and correlation with FEA predicted distortion values.
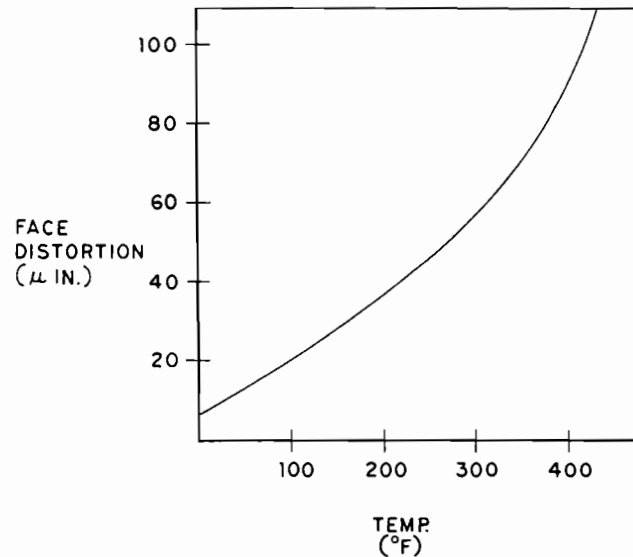

Figure 21. Measured Face Deflection vs Temperature of Welded Metal Bellows Seal.

Optimization of Tribological Characteristics of Seal Face Materials

Although a desired range of mechanical contact pressure (P_{mc}) is used for a seal design, variations of operating conditions and in pressure profile factor K could lead to considerable fluctuations in P_{mc}, as shown in the example in *Hydraulic Balance and Face Loading of Metal Bellows Seals*. Hence, it is necessary to minimize the variation of friction and wear of seal face materials over a wide range of P_{mc}, surface speed, K, fluid viscosity and other operating conditions.

Physical and Microstructural Characteristics

Face material selection for seal applications is often application specific in that material pairs used to generate low friction often exhibit different characteristics than pairs selected for high wear resistance such as in abrasive service conditions. Selection of the proper material pairs depends on the physical properties such as thermal conductivity, density, elastic modulus, hardness, and toughness as well as the microstructural features like grain size, distribution of various phases and porosity, and surface texture.

Based on the thermal expansion coefficient, elastic modulus, thermal conductivity and other empirically determined factors, Mayer [19] tried to define a thermal resistance factor for seal face materials and a selection criteria for dry running conditions. However, the effects of microstructural features and their correlation with tribological properties have not been addressed in the literature. The following discussion of experimental results highlight the importance of microstructural features in controlling the friction and wear of seal face materials.

Hard Face Materials

Three hard face materials are presently being widely used for seal applications. These materials are silicon carbide, tungsten carbide, and aluminum oxide. Typical properties for each is shown in Table 2. Aluminum oxide (Al_2O_3) generally exhibits relatively low hardness compared to silicon carbide, and low thermal shock resistance. Many Al_2O_3 grades exhibit glassy grain boundary phases which wear preferentially and give rise to grain pullout. The pullout phenomenon produces substantial abrasion and high friction for the mechanical seal (Figure 22).

Table 2. *Physical Propertyies of Hard Face Materials for Seal Applications.*

Physical Properties	Materials			
	Al_2O_3	WC	RB SiC	S Sic
Density (gm/cc)	3.9	15.0	3.1	3.1
(lbs/in^3	(0.14)	(0.54)	(0.11)	(0.11)
Elastic Modulus (G Pa)	340	600	380	410
(M psi)	(49)	(87)	(55)	(59)
Thermal Conductivity (W/m K)	13-30	35-80	105-130	100-125
(BTU/h ft °F)	(7.5-17.3)	(20.2-46.8)	(60.7-75.2)	(57.8-72.3)
Hardness (Hv) Kgm/mm^2	1500	1650	2500	2800
KI$_c$ (M Pa $\sqrt{m}$)	4	7	5	4

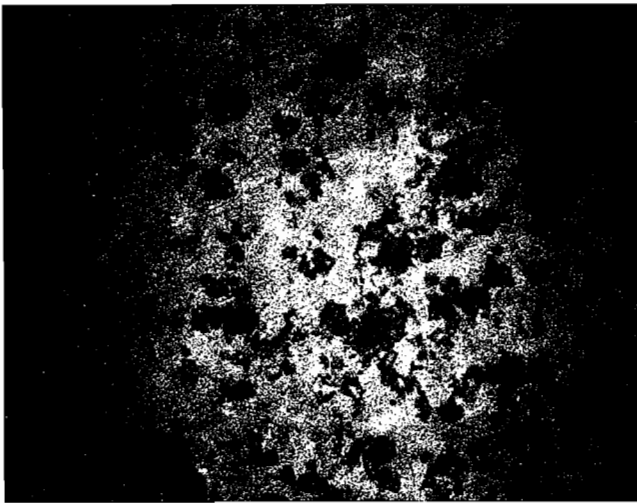SOURCE: Reference 20—E. Meyer & Manufacturers' Data

Figure 22. *Polished Microstructure of Al_2O_3 Showing Pull Out of Large Grains (400 ×).*

Tungsten carbide (WC) is a tough, abrasion resistant material which is heavy, having a density of 0,54 lb/in^3 (15 gm/cc). Its thermal conductivity is somewhat higher than that of Al_2O_3 and is manufactured by sintering tungsten carbide particles into a matrix of nickel or cobalt which acts as the binder. The performance of WC depends greatly on the size of the particles and on the distribution and type of binder used [20]. Tungsten carbide exhibits superior performance in abrasive media applications,
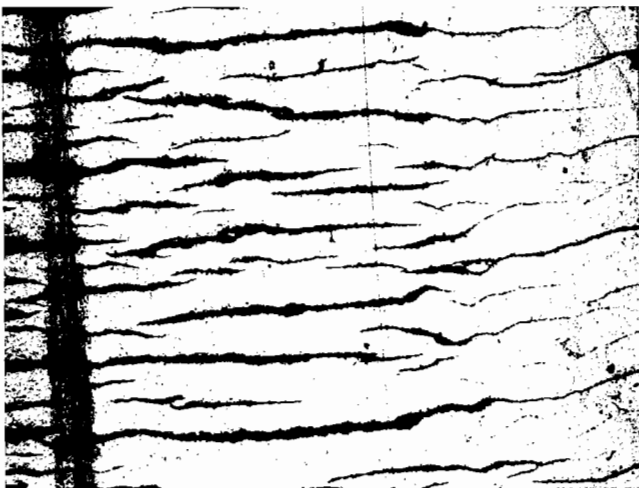

Figure 23. *Optical Micrograph of Heat Checking in WC (50 ×).*

especially running against silicon carbide, but should not be used in high speed applications where excessive heat can be generated at the interface giving rise to thermal cracks at the surface (Figure 23). Use of a higher thermal conductivity material in contact with tungsten carbide such as silicon carbide or some metal impregnated grades of carbon can reduce the thermal cracking problem.

Silicon carbide is a light weight material with a density of 0.11 lb/in^3 (3.1 gm/cm^3) which exhibits high hardness and excellent thermal conductivity. Two general types of silicon carbides, generally used for fluid sealing, are reaction bonded and sintered. The reaction bonded materials exhibit a two phase microstructure, in that silicon carbide particles are surrounded by free silicon. The siliconizing process limits the porosity of the material by adding free silicon which may offer certain advantages in seal applications. However, the free silicon is more susceptible to attack by corrosion and erosion, and applications of reaction bonded materials must be chosen carefully. The sintered SiC is a single phase polycrystalline material containing no free silicon. This material exhibits excellent corrosion resistance and should be used in corrosive applications, but it is also brittle and must be handled carefully.

Good specifications must be developed and rigid quality control programs need to be followed to insure that high quality face materials are used routinely for fluid sealing. Lack of adequate process control causes macroscopic defects such as silicon streaks (Figure 24) or structures with excessive grain growth (Figure 25). The presence of impurities and defects significantly detracts from the desirable wear and friction behavior of a mechanical seal.
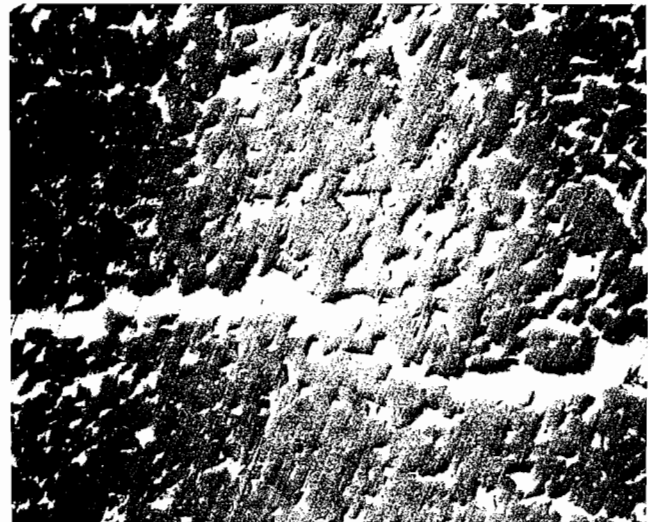

Figure 24. *Optical Micrograph (400 ×) of Silicon Streaking in Reaction Bonded SiC.*

Some suppliers consistently provide high quality SiC with high purity and homogeneous phase distribution as shown in Figure 26. The benefits of superior material quality become evident through lower friction, longer service life, and consistent performance.

Because of superior tribological properties, silicon carbide and carbon graphite pairs are now being most widely used for pump sealing applications, excluding erosive environments. The following study is directed towards optimizing microstructural features of commercially available grades of SiC running against a standard carbon graphite.

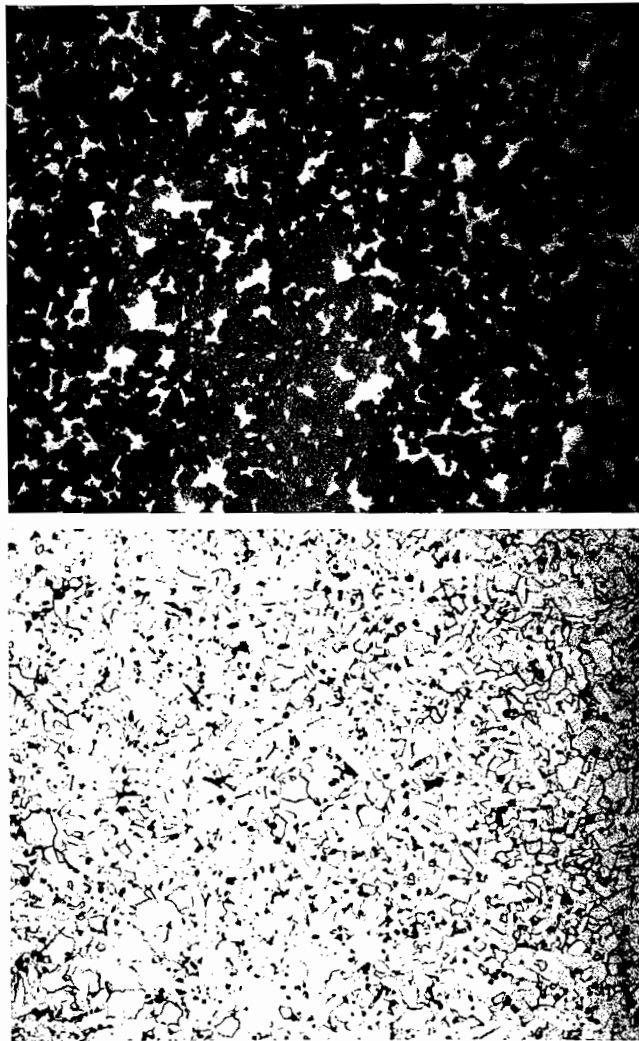Figure 25. Optical Micrograph (400 ×) Showing Grain Growth in Sintered SiC.

Figure 26. Optical Micrographs (400 ×) of Sintered and Reaction Bonded Silicon Carbides, Respectively Showing Good Homogeneity, Proper Distribution of Phases and Small Grain Structure.

Tribological Studies of SiC/CG

This study examines the friction behavior of four commercially available grades of silicon carbide sliding against a standard carbon graphite, using lubricated sliding conditions. Three of the silicon carbide test materials are reaction bonded grades (A, B, and C) and one is a sintered grade (D). The microstructural features are summarized in Table 3, and shown in Figure 27.

Table 3. Microstructural Features of Various Grades of Silicon Carbide Used in the Study.

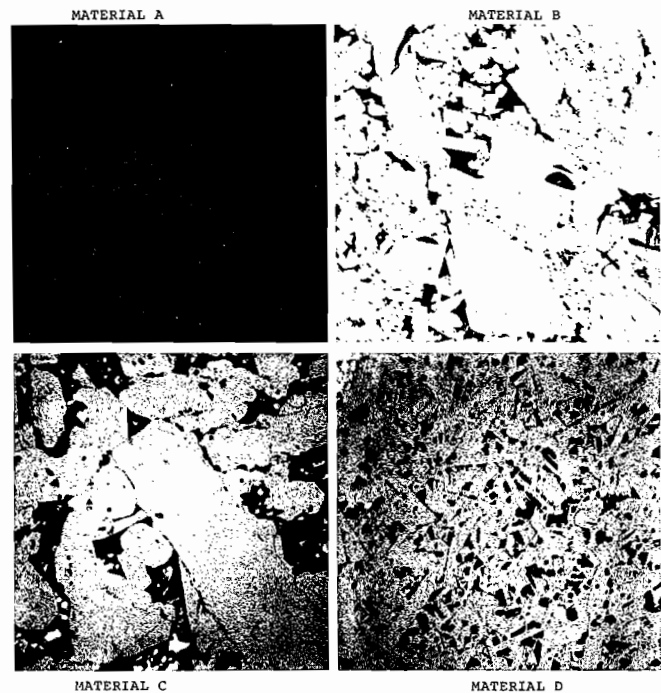| Grade	Type	Average Grain Size	Free Silicon (% Vol.)
A	Reaction Bonded	3 μm	17%
B	Reaction Bonded	Bimodal, 10 μm and 70-100 μm	15%
C	Reaction Bonded	Bimodal, 10μm and 70-100 μm	7%
D	Sintered	7 μm	—

Figure 27. Optical Micrographs (400 ×) Showing the Etched Microstructures of the Reaction Bonded Silicon Carbide A, B, and C and the Sintered Silicon Carbide D.

Tribological testing was conducted in a water lubricating condition using sliding velocities up to 15.4 ft/sec and hydraulic pressures up to 300 psi, producing mechanical contact pressures (P_{mc}) from 35 to 90 psi, for durations of six hours. Frictional torque values and temperature were monitored during the test. Changes in surface texture were determined as a function of running time and the wear tracks were examined using scanning electron microscopy.

The test pieces were designed to have a hydraulic balance of 70 percent. Using the Equation (2), contact pressures are calcu-

lated assuming a linear pressure drop across the seal dam (K = 0.5), and friction coefficients can be estimated from the measured torque values.

Results and Discussion

Friction data for the "B" material at various pressures are presented in Figure 28 as a function of sliding velocity. The frictional torque is shown to increase with pressure but decrease with velocity. The fluid pressure acts to force the seals together and increase the asperity contact. However, the effect of pressure on the corresponding torque becomes less discernible at higher sliding velocities, primarily due to the enhanced fluid film formation, created by the higher speed and the corresponding reduction in the asperity interaction at the seal interface [21, 22]. It is interesting to note that a fifteen fold reduction in pressure produces the same relative drop in friction as 6.4 fold increase in the sliding velocity. Similar trends in frictional torque are observed for the other materials tested.
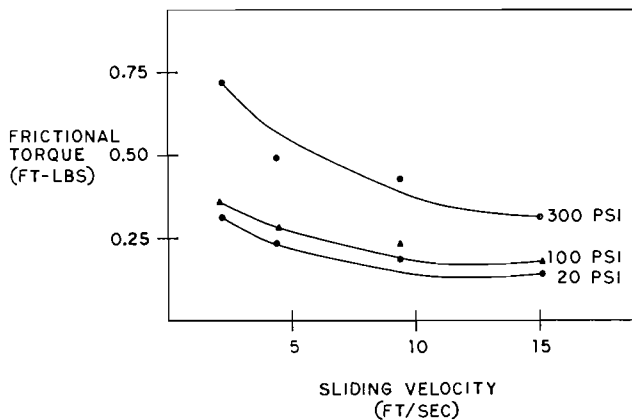

Figure 28. Frictional Torque as a Function of Sliding Velocity for Material "B."

For a sample of material "B," a typical profilometry trace of the lapped surface is shown in Figure 29. The wear surface is illustrated in Figure 30 after a running period of three hours. By comparing the profilometry traces before and after wear, significant asperity shearing can be observed. The associated Ra, which is a measure of average roughness, is smaller for the wear surface and the (skewness) Rsk has a lower value, indicating a decrease of the ratios to peaks to valleys [23]. Removal of the highest asperity peaks during wear causes the symmetry of the amplitude distribution function to change and causes the skewness function to become more negative assuming that the depths of the negative asperities remain unchanged.

To compare the behavior of the four test materials, the power dissipation values at 10.2 ft/sec (2000 rpm) are illustrated as a function of the fluid pressure (Figure 31). Material "A" yields the lowest power dissipation and has less dependence on the fluid pressure than the other materials tested. Material "B" has the highest power dissipation and a higher dependence on the fluid pressure than that of "A." The slope of the power dissipation function is an important parameter because it is believed that the rate of change of the power dissipation with respect to the pressure is related to the degree of asperity interaction and the energy absorbed during asperity shearing. Referring to grain size values as shown in Table 3, it can be recognized that the materials with larger grains exhibit higher friction torque values.
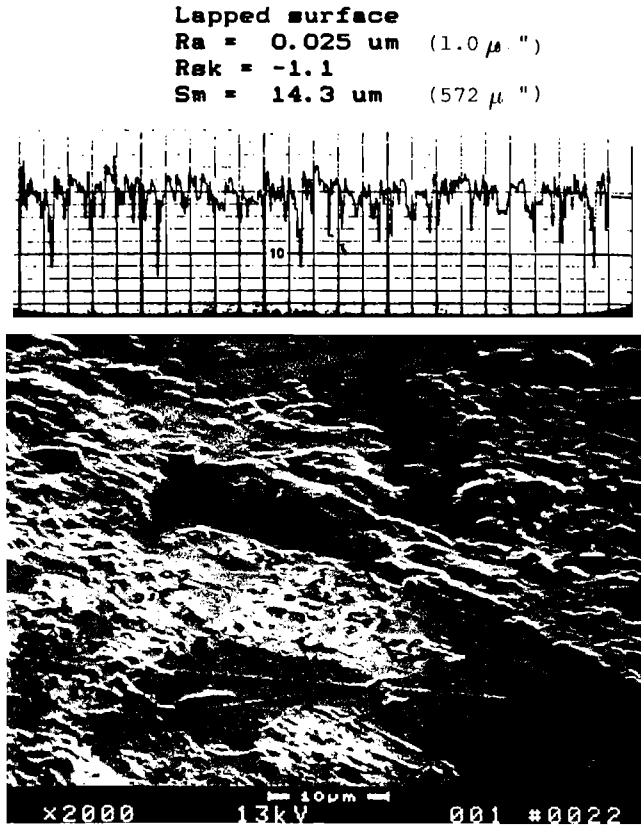
Lapped surface
Ra = 0.025 um (1.0 μ ")
Rsk = -1.1
Sm = 14.3 um (572 μ ")

Figure 29. Profilometry Trace and Scanning Electron Micrograph (2000 ×) of the Lapped Surface for Material "B."

Wear surface
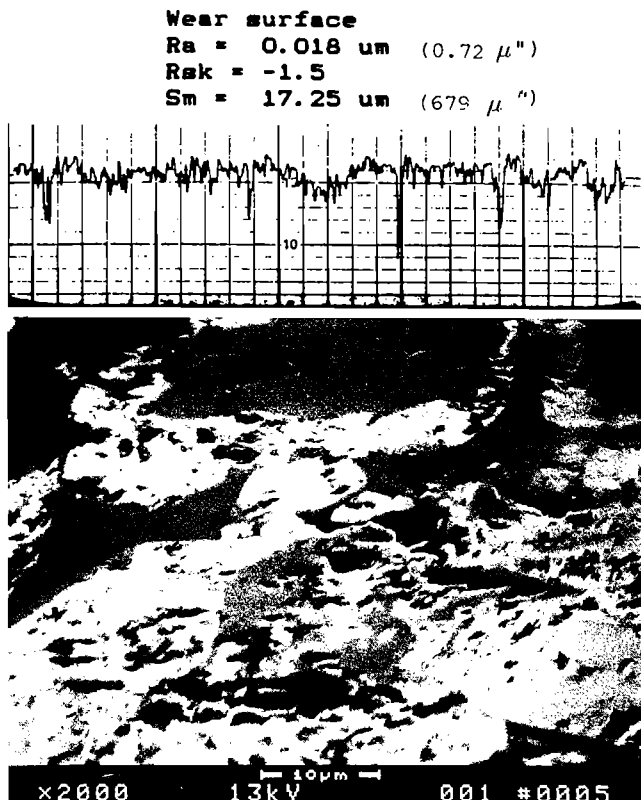Ra = 0.018 um (0.72 μ")
Rsk = -1.5
Sm = 17.25 um (679 μ ")

Figure 30. Profilometry Trace and Scanning Electron Micrograph (2000 ×) of the Wear Surface for Materials "B."
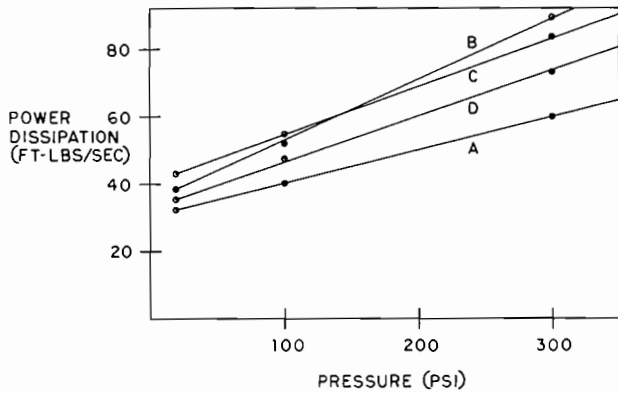
Figure 31. Power dissipation as a function of Pressure for Various Materials.

To compare the friction of various grades and to evaluate the effects of grain size, the reciprocal torque values at a particular surface speed and pressure are plotted as an inverse function of the square root of the grain size (Figure 32). A linear relationship is observed between the SiC grain size and frictional torque. Thus, the inverse of frictional torque or friction coefficient observed in these tests tends to follow the classic Hall-Petch type grain size dependence. It is interesting to note that, frictional torque was somewhat independent of free silicon. Sample "D" with no free silicon but a smaller grain size exhibited a lower frictional torque than "B" with 15 vol percent free silicon but a larger grain size.
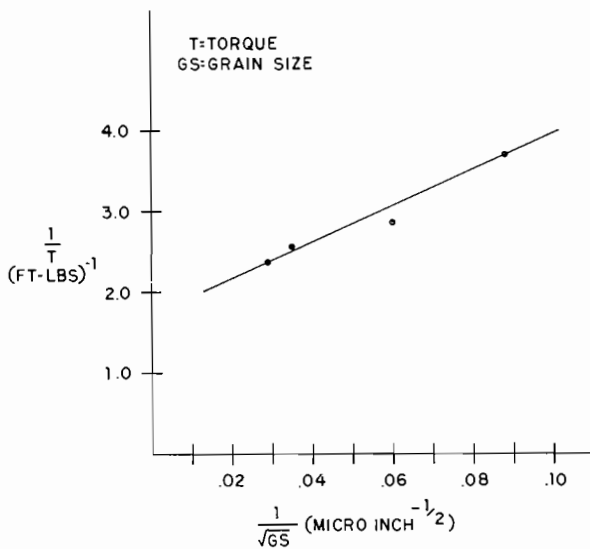

Figure 32. Hall-Petch Plot of Reciprocal Torque for Various SiC Materials.

The Hall-Petch type behavior has been observed by other authors relating the grain size to various properties such as hardness and wear resistance [24, 25, 26]. The grain size dependence of friction can be explained by assuming transgranular fracture at the sliding interface. The roughness of the fractured surface increased with the grain size, thereby, raising the friction coefficient.

CONCLUSIONS

Using experimentally determined bellows force vs. pressure curves, and assuming approximate values of face pressure profile (K), metal bellows seals can be designed to achieve a desired seal face contact pressure (P_{mc}).

To enhance metal bellows fatigue strength and manufacturability, the optimum plate shape for externally pressurized bellows seals consists of a near −45 degree tilt edge at bellows ID and a straight edge at OD.

Two-ply bellows seals exhibit lower spring rates and higher static burst pressures than those of similar single-ply bellows seals with twice the plate thickness. Hence, two-ply bellows seals are preferred in high pressure applications.

For shrinkfit shell insert assemblies, the seal face distortion and the attendant variation of face pressure profile (K) stems predominantly from the relaxation of shrinkfit stresses under operating conditions. Using Finite Element Analysis, the shell insert design can be optimized to minimize this face distortion.

Tribological properties of silicon carbide (SiC) running against carbon graphite are found to depend on the grain size of SiC. The frictional torque values decrease with the SiC grain size. Hence, strict microstructural control is necessary to ensure a fine SiC grain size and eliminate other structural defects like large grains, silicon streaks and excessive porosity.

REFERENCES

1. "Sealol Balanced Pressure Bellows Seals," Sealol Corporation Advance Bulletin 18 (October 1957).

2. Smith, P. E., "Welded Metal Bellows Seals: Applications and Problems," Hydrocarbon Processing, p. 87 (January 1983).

3. Crane Packing Company Bulletin S-205-16.

4. O'Dell, C. W., Wickersham, C. P., and Gaines, A., "SiC Face Bellows Seals in Critical Process Pumps Will Save $25,000/year," Chemical Processing Magazine, (February 1983).

5. Jones, H. H., and Molnar, J., "Metal Bellows Seal Has Extended Life in High Temperature Application," Plant Services Magazine, p. 24 (September 1987).

6. Weichman, H., and Molnar, J., "Abrasive Nitric Acid Slurry Withstood by Bellows Pump Seal with Fluorocarbon O-rings," Plant Services Magazine (September, 1985).

7. Staff, Chemical Processing, "Low-Cost Metal Bellows Seals in Acid and Slurry Pumps Save $10,000 in Maintenance," Chemical Processing Magazine (May 1983).

8. Knowles, B., Burrell, C., and Stadig, W. P.," Metal Bellows Pump Seals are Effective with Difficult Fluids," Chemical Processing Magazine (December 1986).

9. Martel, Y., Botte, J. M., and Regazzacci, P., "Reduce Costs With Metal Bellows Shaft Seals," Hydrocarbon Processing, p. 39 (October, 1987).

10. Buchter, H. H., *Industrial Sealing Technology*, New York: John Wiley and Sons (1979).

11. Bellows Design Guide, EG&G Sealol.

12. Hulbert, L. E., et al. "Final Report on the Development of Analytical Techniques for Bellows and Diaphragm Design," AFRPL-TR-68-22, (March 1968).

13. Hulbert L. E. et al., "Final Report on the Development of the Tilt-Edge Bellows Concept," AFRPL-TR-70-115 (October 1970).

14. Krokel, R., "Laminated Metallic Bellows," U.S. Patent No. 3,090,403, (May 1963).

15. Luxford, G., "Mechanical Face Seals," UK Patent No. 20826938, (June 1984).

16. *Welding Handbook*, American Welding Society, Seventh Edition, 2 (1978).

17. Plumridge, J. P., "Low Cost Metal Bellows Sealing," World Pumps, (April 1987).

18. U.S. Patents #3,658,349 (1972), #4,163,563 (1979).

19. Mayer, E., *Mechanical Seals,* Newnes-Butterworth, (1977).

20. Klimek, E. J., "Selection, Properties and Quality Assurance of Face Materials for Rotating Mechanical Seals," Presented at ASLE-ASME Tribology Conference, San Antonio, Texas (October 1987).

21. Labus, T. J., "The Influence of Rubbing Materials and Operating Conditions on the Power Dissipated by Mechanical Seals," Lubr. Eng., 37, (7), pp. 387-394 (1981).

22. Paxton, R. R. and Hulburt, H. T., "Rubbing Friction in Radial Face Seals," Lubr. Eng., 36, (2), pp. 89-97, (1980).

23. Derby, J. and Hilaris, J., "The Tribological Behavior of Silicon Carbide and Carbon Pairs in Mechanical Face Seal Applications," Presented at ASLE Meeting, Pittsburgh, Pennsylvania (1986).

24. Wu, C. C., Rice, R. W., Johnson, D., and Platt B. A., "Grain Size Dependence of Wear in Ceramics," Proceedings of the 9th Annual Conference on Composites and Advanced Ceramic Materials, Cocoa Beach, Florida, American Ceramic Society, Columbus, Ohio, p. 995 (January 1985).

25. Wu, D. D., Rice, R. W., Platt, B. A., and Carrle, S., "Wear and Microstructure of SiC Ceramics, Proceedings of the 9th Annual Conference on Composites and Advanced Ceramic Materials, Cocoa Beach, Florida, American Ceramic Society, Columbus, Ohio, p. 1023 (January 1985).

26. Rice, R. W., "Micro Mechanics of Microstructural Aspects of Ceramic Wear," Proceedings of the 9th Annual Conference on Composites and Advanced Ceramic Materials, Cocoa Beach, Florida, American Ceramic Society, Columbus, Ohio, p. 94 (January 1985).